

Compact, diode-pumped, unstable cavity Yb:YAG laser and its application in laser shock peening

Körner, J., Zulić, S., Reiter, J., Lenski, M., Hein, J., Bödefeld, R., Rostohar, D., Mocek, T. & Kaluza, M. C

Published PDF deposited in Coventry University's Repository

Original citation:

Körner, J, Zulić, S, Reiter, J, Lenski, M, Hein, J, Bödefeld, R, Rostohar, D, Mocek, T & Kaluza, MC 2021, 'Compact, diode-pumped, unstable cavity Yb:YAG laser and its application in laser shock peening', Optics Express, vol. 29, no. 10, 423386, pp. 15724-15732. <https://doi.org/10.1364/OE.423386>

DOI 10.1364/OE.423386

ISSN 1094-4087


Publisher: Optica

An OSA-formatted open access journal article PDF may be governed by the OSA Open Access Publishing Agreement signed by the author and any applicable copyright laws. Authors and readers may use, reuse, and build upon the article, or use it for text or data mining without asking prior permission from the publisher or the Author(s), as long as the purpose is non-commercial and appropriate attribution is maintained.

European Regional Development Fund (CZ.02.1.01/0.0/0.0/15_006/ 0000674); Horizon 2020 Framework Programme (739573); Thüringer Ministerium für Wirtschaft, Wissenschaft und Digitale Gesellschaft (2016FE9058); Laserlab-Europe (654148); Bundesministerium für Bildung und Forschung (03VNE2068D, 03Z1H531, 03ZIK445, 05P15SJFA1).



Compact, diode-pumped, unstable cavity Yb:YAG laser and its application in laser shock peening

JÖRG KÖRNER,^{1,2,*}  SANIN ZULIĆ,³ JÜRGEN REITER,^{1,2} MATHIAS LENSKI,¹ JOACHIM HEIN,^{1,2} RAGNAR BÖDEFELD,⁴ DANIJELA ROSTOHAR,² TOMÁŠ MOCEK,² AND MALTE C. KALUZA^{1,2}

¹*Institute of Optics and Quantum Electronics, Friedrich-Schiller University, Max-Wien Platz 1, 07743 Jena, Germany*

²*Helmholtz Institute Jena, Fröbelstieg 3, 07743 Jena, Germany*

³*HiLASE Centre, Institute of Physics of the Czech Academy of Sciences, Za Radnicí 828, 252 41 Dolní Břežany, Czech Republic*

⁴*Lastronics GmbH, Moritz-von-Rohr-Str. 9, 07745 Jena, Germany*

*joerg.koerner@uni-jena.de

Abstract: We present the setup of a compact, q-switched, cryogenically cooled Yb:YAG laser, which is capable of producing over 1 J output energy in a 10 ns pulse at 10 Hz. The system's design is based on the recently published unstable cavity layout with gain shaping of the spatial intra-cavity intensity distribution. Using a hexagonal homogenized pump beam, the laser generated an according hexagonal output beam profile. The suitability of such laser properties for the intended use in a laser shock peening process is demonstrated. In the experiment an aluminum plate was treated and the generated residual stresses in the sample subsequently measured. Other applications of this laser system like laser pumping or surface cleaning are conceivable.

© 2021 Optical Society of America under the terms of the [OSA Open Access Publishing Agreement](#)

1. Introduction

Nanosecond high energy class laser systems are an essential prerequisite for many demanding applications. In particular systems based on neodymium doped laser media are used for a wide range of applications. In combination with frequency doubling such lasers are used as a pump source for high intensity titanium sapphire laser systems [1], which are widely used in science. Industrial applications, such as laser shock peening (LSP) rely both on the availability and reliability of such systems [2]. Furthermore, the process of LSP is being used in a broader variety of applications, e.g. in combination with 3D-printing [3]. In medicine, such laser systems are important e.g. for tattoo removal treatment [4]. The list of currently realized and future applications could be expanded much further.

Such high energy class laser systems typically operate in the wavelength range close to 1 μm . Most of these systems are based on neodymium doped active media. A major reason for the dominance of neodymium doped media is their compatibility with laser diode pumping, which reduces thermal load, and a relatively high optical gain significantly simplifying the complexity of the layout of the amplifiers. Nevertheless, in high repetition rate lasers, based on fiber or thin-disc technology, ytterbium doped active media are dominating due to their intrinsically lower quantum defect, their even better spectral compatibility with high power diode lasers and their very high quantum efficiency. During pulse-pumped operation of ytterbium lasers, as required for high energy pulse generation, the relatively low emission cross sections and re-absorption present at room temperature, require suitable countermeasures in the design. Therefore, such lasers typically feature highly complex layouts that are only affordable in scientific applications and therefore prohibiting their wide spreading. Nevertheless, scientific systems have already

demonstrated highly efficient generation of pulse energies in excess of 100 J at 1 kW average power, while maintaining good beam quality [5].

A common mitigation strategy for the re-absorption effect in ytterbium-doped laser media is to cryogenically cool the active medium and thereby thermally depopulating the lower laser levels and increasing the peak cross sections [6]. As a positive side effect also the thermo-mechanical properties tend to be more favorable under these conditions in many host materials [7].

Furthermore, the low gain requires concepts for providing a high number of material passes without drastically increasing the system's optical complexity. While resonators and regenerative amplifiers relying on a stable cavity layout are well suited for output pulse energies in the mJ range, such setups are problematic for larger mode sizes, that are required for higher energies to avoid laser induced damage.

Hence, for high energy amplifiers multi-pass layouts are commonly used. To maintain a high beam quality such layouts require an imaging system between individual material passes. For attaining a relatively high number of passes so called relay imaging setups can be utilized [8]. Though such setups reduce the system's complexity and the number of optical elements, several subsequent amplifier stages are required to achieve a desired output energy when starting at the mJ level.

In our previous work [9] we have demonstrated that by applying a spatial gain shaping, unstable cavity resonators can achieve significantly higher intra-cavity feedback as compared to classical graded reflectivity mirror layouts [10]. This allows the use of an unstable resonator layout with ytterbium gain media as well. In comparison to stable resonators the mode sizes in such setups are not generally limited and they therefore, in principle, allow for the direct generation of multi-Joule output pulses even in a q-switched mode. The scheme could drastically reduce the complexity of high energy ytterbium lasers either by avoiding multi-pass amplifier stages completely or at least through reducing the gain to be achieved by these significantly.

In this work we present the energy scaling of our previous setup [9] to more than 1 J output energy in an approximately 10 ns long pulse, that is directly generated in the q-switched unstable cavity laser. Major improvements include an increased pump peak power to approximately 7 kW in a homogenized hexagonal tophat beam and a cryogenically cooled ceramic Yb:YAG active medium with Cr⁴⁺ absorber cladding for the suppression of amplified spontaneous emission and transverse lasing.

With this system we could demonstrate a high optical to optical efficiency of up to 37 %. Pulse energies in excess of 1 J were obtained at a repetition rate of up to 10 Hz. For higher repetition rates of up to 25 Hz the system is still operable, though the cooling power of our cryostat limits the performance.

The system's potential for its application in laser shock peening was tested by treating an aluminum alloy sample and evaluating the generated residual stress using the hole drilling method. The observed induced residual compressive stress in the order of 200 MPa proves the suitability of our approach for such an application. The combination of compact footprint, simple architecture, and high efficiency of this approach underline its potential to be used in future industrial laser systems.

2. Laser setup

The laser setup as shown in Fig. 1 follows basically our previous work [9]. The unstable cavity consists of a convex mirror (CXM) with 4 m radius of curvature and a concave mirror (CCM) with 5 m radius. Both mirrors have a high reflective coating (better than 99.5% reflectivity) for the laser wavelength. The resulting cavity length is 0.5 m and the round trip magnification 1.25. The mode shaping, which is based on gain shaping, was already described in [9].

The output coupling was realized using a thin film polarizer (TFP) with an angle of incidence of 56° in combination with a quarter wave plate ($\lambda/4$) and a KD*P Pockels cell (IMPACT13,

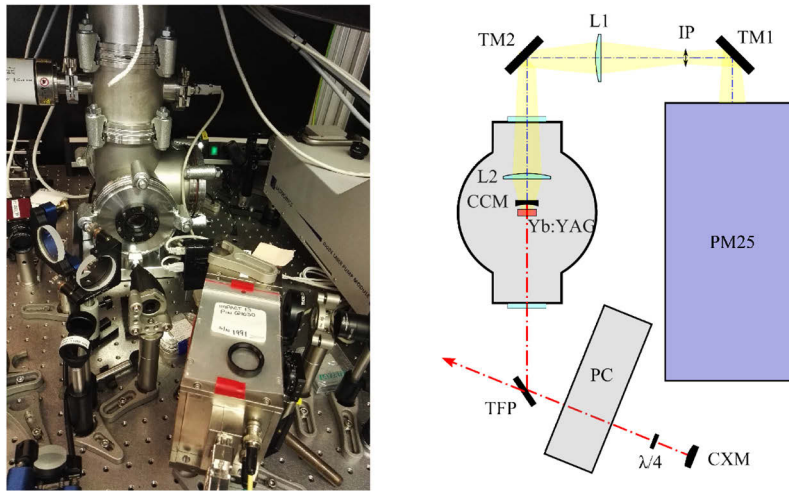


Fig. 1. Left: Laboratory setup of the laser. The vacuum chamber of the cryostat can be seen in the upper left part, the pump module on the right side. In the foreground the Pockels cell housing is shown. Right: Schematic setup of the laser system. It is: CCM: concave mirror with radius 5 m, CXM: convex mirror with radius 4 m, IP: intermediate image plane of the homogenized pump beam, L1 and L2: lenses, PM25: diode laser pump module, $\lambda/4$: quarter wave plate, TFP: thin film polarizer, TM1 and TM2: turning mirrors.

Gooch & Housego PLC) (PC). The cavity is blocked if no voltage is applied to the Pockels cell. By adjusting the PC on-voltage amplitude the output coupling could be adapted to maximize the output pulse energy in q-switched operation.

The laser diode pump engine (PM25, *Lastronics GmbH*) generated a hexagonal tophat beam with up to 7 kW peak power. Its output beam profile is re-imaged with lenses L1 and L2 onto the active medium with the short diagonal being approx. 5 mm, resulting in an illuminated area of approximately 0.22cm^2 . This generates a gain profile of similar size, which also defines the cavity's mode shape. The pump beam is coupled into the laser cavity via the CCM, which additionally acted as a dichroic mirror with anti-reflective coating for the pump wavelength and high reflectivity at the laser wavelength.

The laser medium, which is placed close to the CCM, is an 8 mm thick and 28 mm diameter ceramic YAG disc, with 2 at.% ytterbium doping in the central area up to a diameter of 20 mm. The outer ring shaped area is doped with 0.25 at.% chromium ions (Cr^{4+}). It absorbs the ytterbium fluorescence and therefore effectively suppresses transverse amplified spontaneous emission and self lasing, which would otherwise limit the performance of the laser (cf. [9]). The laser medium was anti-reflection coated for both laser and pump wavelengths. For cooling, the crystal is clamped on the front and back-side close to its circumference in a gold plated copper holder directly attached to the cold finger of a bath cryostat. To establish the thermal contact a ring of indium foil was used on both sides. By this clamping method radial stress due to expansion mismatch could be avoided effectively, while a reasonable thermal connection was achieved. The cooling setup is shown in Fig. 2. For thermal insulation and to avoid condensation the laser crystal and neighboring optics were enclosed in a vacuum chamber at a pressure of less than 10^{-6} mbar.

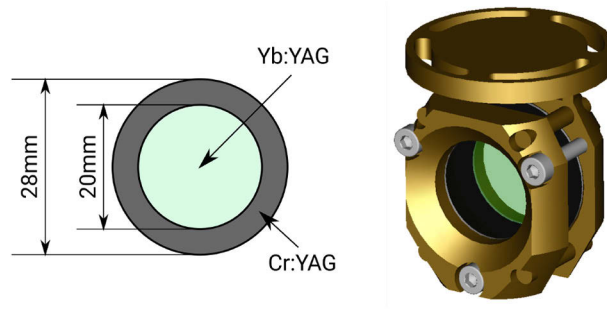


Fig. 2. Left: Layout of the used Yb:YAG ceramic with Cr:YAG cladding. Right: Yb:YAG ceramic with chromium cladding mounted in the copper holder. The mount is attached to the cold finger of a bath cryostat on the top side.

3. Laser results

The output performance of the laser under q-switch operation as a function of the pump pulse duration is shown in Fig. 3. During this measurement the active medium was cooled down to a temperature of 78 K and the lasers repetition rate was set to 2 Hz, to avoid strong influence of the heating. The voltage applied to the Pockels cell was regulated during the measurements to optimize for maximum energy output, also yielding a nearly symmetrical, Gaussian like temporal output pulse shape with variable pulse duration. The design value of 1 J per pulse was reached for a pump duration of approximately 750 μ s. With longer pump duration, the output energy was further increased to a maximum of 1.14 J. As the slope of the curve describing the extracted laser energy becomes relatively flat for longer pump duration. As the pump pulse duration is still in the range of the fluorescence lifetime of 950 μ s, this indicates that despite the absorbing cladding the high gain in the material likely limits the energy storage capability due to the generation of amplified spontaneous emission.

The duration of the output pulse was measured using a photodiode (DET10A2, Thorlabs inc.) and an oscilloscope with 500 MHz bandwidth (MSO7054, RIGOL Technology Co., Ltd.). For a pump duration longer than 500 μ s the full width at half maximum output pulse duration was nearly constant in the range from 9 ns to 12 ns, with slightly shorter pulses for longer pump pulse duration and higher output energy. This duration corresponds to about two cavity round-trips.

In the configuration used the match between the absorption of Yb:YAG and our pump source was not ideal as the center wavelength of the pump module was about 931 nm, at which the absorption cross section is only about half of its maximum value near 941 nm. Nevertheless, as the absorption spectrum is relatively flat in the spectral range from 925 nm to 935 nm, a thermally induced drift of the pump module's emission wavelength due to a changing heat load does therefore not significantly alter the absorption and therefore will not affect the lasers stability.

The saturation intensity I_{sat} at the pump wavelength λ_p can be calculated using:

$$I_{sat} = \frac{hc}{\lambda_p \tau_f \cdot (\sigma_a(\lambda_p) + \sigma_e(\lambda_p))} \quad (1)$$

Here, h is the Planck constant, c the speed of light, τ_f the fluorescence lifetime and σ_a and σ_e the cross section for absorption and emission on the pump wavelength respectively. Using the spectroscopic values given in [11] we obtain $I_{sat} \approx 47$ kW/cm² for our pump wavelength. As the pump intensity is only about 20 kW/cm² the spectral absorption can be approximated using Lambert Beer's law. The accordingly calculated spectrum of the pump pulses transmitted through the active medium for operation at 2 Hz and 10 Hz is shown in Fig. 4. The absorption of the pump was calculated to be about 63 %, independent on the repetition rate. This allows to

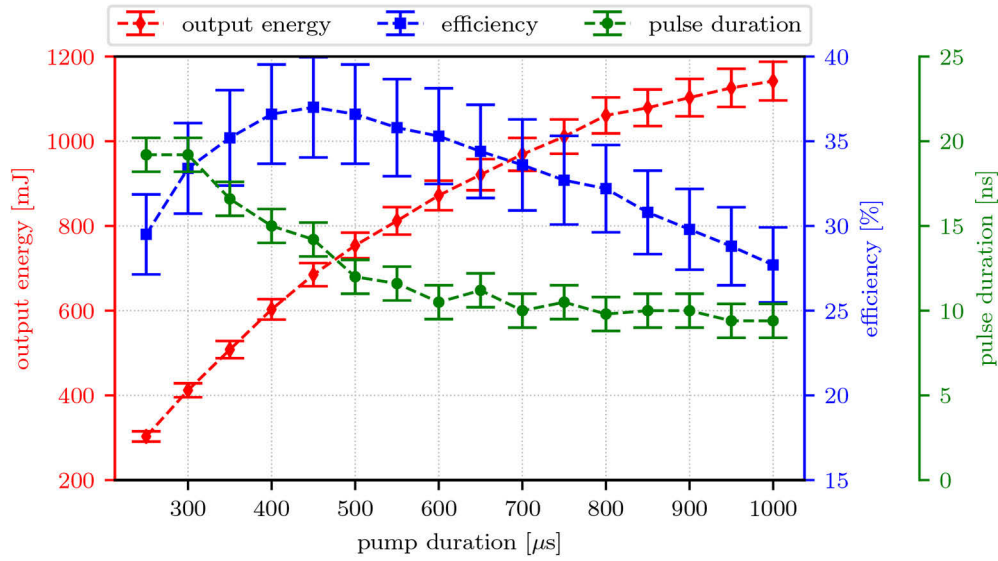


Fig. 3. Output energy (red), optical to optical efficiency with respect to absorbed pump energy (blue) and output pulse duration (green) as a function of pump pulse duration. The laser was operated at a repetition rate of 2 Hz. The pump diode module's peak power was set to 6.375 kW. The active medium's temperature was kept at approx. 78 K.

calculate the absorbed pump energy E_{pa} in the active medium. With the laser's output energy E_{out} the optical to optical efficiency η_{oo} is calculated by $\eta_{oo} = E_{out}/E_{pa}$.

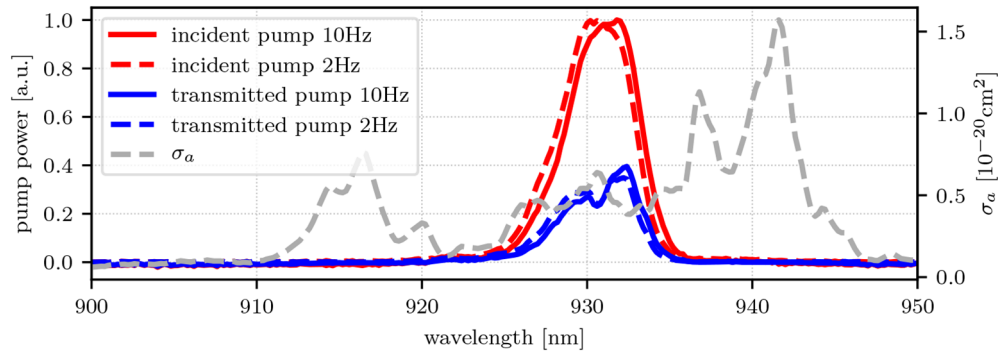


Fig. 4. Spectra of incident (measured) and transmitted (computed using Lambert Beer's law). The dashed grey line shows the according absorption cross sections for Yb:YAG at 80K (data taken from [11]).

The highest efficiency of 37 % was obtained with a pump duration of 450 μs and an output energy of 0.685 J. For longer pulses the efficiency slightly dropped, though even at 1 J output energy the efficiency was larger than 32 %.

The output beam profile (cf. Figure 5) was measured in an image plane of the active medium outside the cavity. It resembles a hexagonal tophat profile, as given by the pump module's intensity distribution. The wings as predicted by the theoretical model in [9] are not significant, which is attributed to the relatively high gain. Using a numerical model solving the rate equations with the cross sections given in [11] for 77K the small signal gain per round-trip (double pass)

was estimated to be in the range from 25 to 50. Residual features as well would be truncated by the limiting apertures in the setup especially of the Pockels cell.

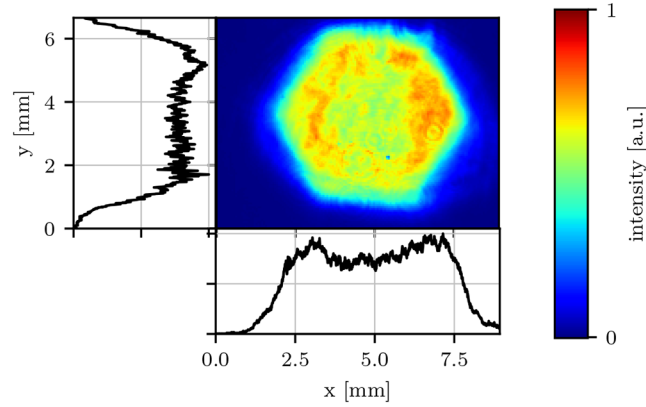


Fig. 5. Measured output beam profile for approx. 1 J output energy. The graphs at the side correspond to the according lineouts through the beam's center.

Furthermore, we investigated the average power capability of the system by increasing the repetition rate, while keeping the other settings unchanged. The laser was operated with a pump duration of 850 μs corresponding to about 1 J of output energy as determined before. As shown in Fig. 6, the output energy is nearly constant for a repetition rate of up to 10 Hz. When further increasing the repetition rate the output power starts to drop. At 25 Hz, still an output energy of 750 mJ is obtained. The drop in energy is linked to a strong increase in the temperature of the crystal holder. During these experiments the output profile of the laser showed no signs of degradation. This indicates an insufficient cooling capacity of the bath cryostat. At 25 Hz a temperature increase of 25 K with respect to the temperature with no thermal load was measured. Therefore, using a cooler with higher capacity is expected to allow for a higher repetition rate at nearly constant output pulse energy.

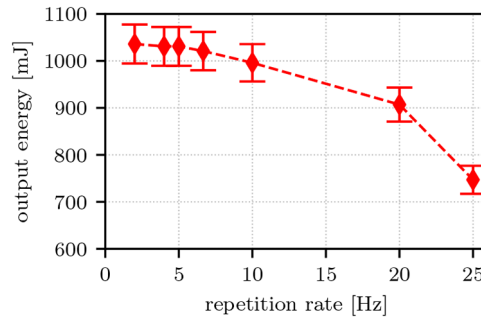


Fig. 6. Output energy as a function of the repetition rate.

4. Laser shock peening experiment

As a proof of principle test for the applicability of the system to the laser shock peening process, a simplified treatment setup was employed. As the oscillator's output coupling is in diverging beam direction, the beam was first collimated using a 5 m radius spherical mirror. A 1 m focal length lens was then used to generate a de-magnified image of the intra-cavity intensity distribution

with a beam diameter of 2.6 mm, resulting in a fluence of 33 J/cm^2 , which corresponds to approximately 3 GW/cm^2 on the target.

The final lens was mounted on an x-y stage together with additional turning mirrors, allowing to move the beam's position on the target, so that the target position could be kept fixed. Though the movement of the stage changes the distance to the object plane by a few centimeters, the feedback of this with respect to image distance and image size was not significant due to the long object distance of approximately 4.5 m. The final beam was pointed directly downwards onto the sample under only a small angle with respect to the vertical direction to avoid direct back-reflection into the laser.

The sample we used was an aluminum alloy (EN AW 7075) plate of 5 mm thickness and dimensions of 100 mm by 100 mm. On the plate, we applied vinyl tape, which is used in LSP processing as a sacrificial layer to prevent surface melting and to prevent the generation of tensile residual stress on the surface. The sample with the applied vinyl tape was immersed in a water filled bowl so the thickness of the water above the sample was approximately 1 mm. The latter is needed to contain the pressure wave generated by the laser induced plasma on the samples surface.

The frequency of the laser for the experiment was limited to 1 Hz, while the shots on the sample were done in single-shot mode. The spatial overlap of laser shots was 50 %. After a line of approx. 20 mm length was processed, further lines with a spacing of 2.25 mm were processed with alternating direction. In the end, the created LSP patch measured approximately 20 mm by 20 mm. A detailed sketch of the treatment pattern is shown in Fig. 7.

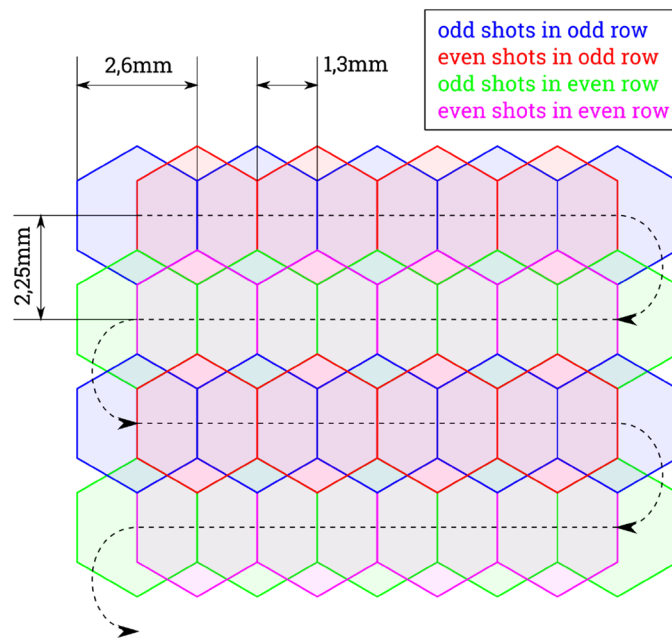


Fig. 7. Treatment pattern during the LSP treatment. The dashed line shows the general beam movement.

For a test of the applicability of the laser system for the LSP processing, we used the laser close to its maximum output energy of 1 J in a pulse on-demand mode for the treatment of an aluminum EN AW 7075 sample. Since the imparted residual stress is the main characteristic of the LSP processing, the sample was subsequently characterized by hole drilling residual stress measurement technique. Measurements were carried out with a Prism hole drilling system

(Stresstech Oy), which is based on electronic speckle pattern interferometry for calculating the residual stresses. The results are presented in Fig. 8.

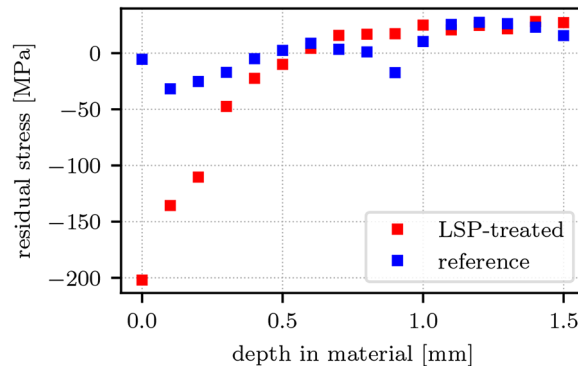


Fig. 8. Comparison of residual stress before and after LSP-treatment as a function of the depth in the material measured with the hole drilling method.

The blue squares represent the reference depth profile before the LSP processing has been applied. As can be seen, the sample was stress released and the residual stress was around 0 MPa throughout the depth of measurement. The red squares represent the depth profile after applying the LSP processing. The compressed residual stresses have been imparted up to 0.5 mm. In general, compressed residual stresses can be of a higher amount and can be imparted deeper into aluminum alloys, but with optimized LSP processes. However, the measured values of 200 MPa, 135 MPa, 110 MPa, etc. of compressed residual stresses after the applied process are significant enough in comparison with the reference values indicating that the laser will achieve the peening effect in an optimized treatment setup.

5. Conclusion

We presented a cryogenically cooled Yb:YAG q-switched laser system with more than 1 J output energy in a 10 ns pulse. For suppression of amplified spontaneous emission, a ceramic laser medium with a Cr:YAG cladding is used. The laser design is based on a single unstable resonator using the gain guiding principle for generating a hexagonal tophat shaped output pulse and allows for a compact setup. In this configuration a very high optical to optical efficiency of up to 37 % is obtained.

Due to its simplicity and compactness the presented system has a significant potential to be developed into a laser for various scientific and industrial applications. As a test case the applicability for LSP treatment was tested achieving reasonable values for the compressive residual stress generated in aluminum alloy EN AW 7075. This indicates, that the proposed system could be well deployed for a compact, high efficient LSP treatment laser system.

Funding. European Regional Development Fund (CZ.02.1.01/0.0/0.0/15_006/ 0000674); Horizon 2020 Framework Programme (739573); Thüringer Ministerium für Wirtschaft, Wissenschaft und Digitale Gesellschaft (2016FE9058); Laserlab-Europe (654148); Bundesministerium für Bildung und Forschung (03VNE2068D, 03Z1H531, 03ZIK445, 05P15SJFA1).

Disclosures. The authors declare no conflicts of interest.

References

1. S. Gales, K. A. Tanaka, D. L. Balabanski, F. Negoita, D. Stutman, O. Tesileanu, C. A. Ur, D. Ursescu, I. Andrei, S. Ataman, M. O. Cernaianu, L. D'Alessi, I. Dancus, B. Diaconescu, N. Djourellov, D. Filipescu, P. Ghenuche, D. G. Ghita, C. Matei, K. Seto, M. Zeng, and N. V. Zamfir, "The extreme light infrastructure-nuclear physics (eli-np) facility: new horizons in physics with 10 pw ultra-intense lasers and 20 mev brilliant gamma beams," *Rep. Prog. Phys.* **81**(9), 094301 (2018).

2. D. Rostohar, J. Körner, R. Bödefeld, A. Lucianetti, and T. Mocek, "How new laser development can help laser shock peening penetration to widen industrial applications?" *2017 IEEE 3rd International Forum on Research and Technologies for Society and Industry (RTSI)* **7**, 1–4 (2017).
3. N. Kalentics, M. O. V. de Seijas, S. Griffiths, C. Leinenbach, and R. E. Logé, "3d laser shock peening – a new method for improving fatigue properties of selective laser melted parts," *Addit. Manuf.* **33**, 101112 (2020).
4. L. I. Naga and T. S. Alster, "Laser tattoo removal: An update," *Am. J. Clin. Dermatol.* **18**(1), 59–65 (2017).
5. P. Mason, M. Divoký, K. Ertel, J. Pilař, T. Butcher, M. Hanuš, S. Banerjee, J. Phillips, J. Smith, M. De Vido, A. Lucianetti, C. Hernandez-Gomez, C. Edwards, T. Mocek, and J. Collier, "Kilowatt average power 100 j-level diode pumped solid state laser," *Optica* **4**(4), 438 (2017).
6. D. C. Brown, "The promise of cryogenic solid-state lasers," *IEEE J. Sel. Top. Quantum Electron.* **11**(3), 587–599 (2005).
7. R. L. Aggarwal, D. J. Ripin, J. R. Ochoa, and T. Y. Fan, "Measurement of thermo-optic properties of $\text{Y}_3\text{Al}_5\text{O}_{12}\text{Y}_3\text{Al}_5\text{O}_{12}$, YAlO_3 , LiYF_4 , LiLuF_4 , BaY_2F_8 , $\text{KGd}(\text{WO}_4)_2$, and $\text{KY}(\text{WO}_4)_2$ laser crystals in the 80–300 K temperature range," *J. Appl. Phys.* **98**(10), 103514 (2005).
8. J. Körner, J. Hein, and M. Kaluza, "Compact aberration-free relay-imaging multi-pass layouts for high-energy laser amplifiers," *Appl. Sci.* **6**(11), 353 (2016).
9. J. Körner, S. Zulić, D. Rostohar, A. Lucianetti, and T. Mocek, "Novel unstable resonator configuration for highly efficient cryogenically cooled Yb:YAG q-switched laser," *Opt. Express* **27**(15), 21622–21634 (2019).
10. M. Morin, "Graded reflectivity mirror unstable laser resonators," *Opt. Quantum Electron.* **29**(8), 819–866 (1997).
11. J. Körner, V. Jambunathan, J. Hein, R. Seifert, M. Loeser, M. Siebold, U. Schramm, P. Sikocinski, A. Lucianetti, T. Mocek, and M. C. Kaluza, "Spectroscopic characterization of Yb^{3+} -doped laser materials at cryogenic temperatures," *Appl. Phys. B* **116**(1), 75–81 (2014).